Molecular Cell
Article

Homologous Recombination in Real Time: DNA Strand Exchange by RecA

Thijn van der Heijden,[1] Mauro Modesti,[2,4] Susanne Hage,[1] Roland Kanaar,[2,3] Claire Wyman,[2,3] and Cees Dekker[1,*]
[1]Kavli Institute of Nanoscience, Delft University of Technology, Lorentzweg 1, 2628 CJ Delft, The Netherlands
[2]Department of Cell Biology and Genetics, Cancer Genomics Center
[3]Department of Radiation Oncology
Erasmus Medical Center, P.O. Box 2040, 3000 CA Rotterdam, The Netherlands
[4]Present address: Genome Instability and Carcinogenesis, CNRS UPR 3081, 31 Chemin Joseph Aiguier, 13402 Marseille Cedex 20, France.
*Correspondence: c.dekker@tudelft.nl
DOI 10.1016/j.molcel.2008.03.010

SUMMARY

Homologous recombination, the exchange of strands between different DNA molecules, is essential for proper maintenance and accurate duplication of the genome. Using magnetic tweezers, we monitor RecA-driven homologous recombination of individual DNA molecules in real time. We resolve several key aspects of DNA structure during and after strand exchange. Changes in DNA length and twist yield helical parameters for the protein-bound three-stranded structure in conditions in which ATP was not hydrolyzed. When strand exchange was completed under ATP hydrolysis conditions that allow protein dissociation, a "D wrap" structure formed. During homologous recombination, strand invasion at one end and RecA dissociation at the other end occurred at the same rate, and our single-molecule analysis indicated that a region of only about 80 bp is actively involved in the synapsis at any time during the entire reaction involving a long (~1 kb) region of homology.

INTRODUCTION

Homologous recombination is an important pathway for accurate repair of DNA double-strand breaks, is required for generating genetic diversity during meiosis, and is essential for overcoming difficulties in replication. The core events of homologous recombination are homology recognition and DNA strand exchange catalyzed by RecA-type recombinases (Wyman and Kanaar, 2004). Bacterial RecA is the most extensively studied recombinase, but similar proteins exist in all kingdoms of life, including eukaryotic Rad51 and archaeal RadA. These proteins work as molecular machines by assembling filaments along one DNA partner that can then exchange the local base pairing with another DNA molecule with the same sequence.

The strand-exchange reaction central to homologous recombination proceeds through the concerted rearrangement of DNA strands catalyzed by the assembly, rearrangement, and disassembly of a RecA-nucleoprotein filament. Determining the structures formed and their dynamic transitions during nucleoprotein-filament invasion of a target duplex DNA is key to understanding the mechanism of strand exchange. Some aspects of these events have been described. Using fluorescence resonance energy transfer to detect association of an invading single-stranded DNA and dissociation of one strand of the double-stranded DNA revealed the detailed kinetics of these two steps (Bazemore et al., 1997a, 1997b; Ellouze et al., 1997; Gumbs and Shaner, 1998). However, changes in DNA structure during exchange were not probed. Other approaches show that the target duplex DNA molecule is partly unwound prior to strand invasion. This is a signature for a mechanism involving the melting and annealing of recombining DNA strands (Zhou and Adzuma, 1997), implying that DNA dynamics, such as transient melting of a few base pairs, is an important aspect of homology recognition (Folta-Stogniew et al., 2004). Indeed, potential base pairing involving all three strands in the exchange reaction appears not to be an important aspect of DNA structure accompanying homology recognition (Frank-Kamenetskii and Mirkin, 1995). However, other aspects of the arrangement of the three participating strands have not been described.

The RecA-mediated association of three DNA strands is required at some point during strand exchange. The strands are likely arranged as a coaxial, stretched, and underwound ternary intermediate (Kiianitsa and Stasiak, 1997). Double-stranded DNA bound by RecA, and similar recombinases, is stretched and unwound in a DNA structure proposed to be intrinsically recombinogenic (Yu et al., 2004). The lack of direct structural information showing the arrangement of single- or double-stranded DNA within a RecA filament or of any structure formed during strand exchange still limits our understanding of this process. Some specific features for a three-stranded helical structure in the presence of RecA have been predicted from molecular modeling simulations (Bertucat et al., 1999). Strand exchange is often described as proceeding from an invading RecA-coated single-stranded DNA arranged in parallel to the duplex DNA forming a so-called paranemic joint that is then converted into a plectonemic joint as the single-stranded DNA forms an interwound structure with the duplex DNA (Bianchi et al., 1983). However, direct evidence for a paranemic joint, a description of the dynamic transition to a plectonemic joint, and the length of DNA involved at either step have not yet been obtained.

To define some of the so far unprobed mechanistic aspects of RecA-mediated strand exchange, we have taken a single-molecule approach. Strand exchange catalyzed by the assembly, rearrangement, and disassembly of RecA filaments is coupled to changes in DNA structure that can be measured and manipulated in magnetic tweezers. We analyzed structural transitions in a target double-stranded DNA molecule during individual defined strand-exchange events in real time. In this way, we obtained direct information on the extent of DNA involved, the changes in DNA structure, and their duration. During joint-molecule formation, a RecA-bound three-stranded intermediate was formed. Subsequently, during strand exchange, the displaced strand was wrapped around the newly formed duplex DNA into a D wrap structure. The synaptic area involved between the invading nucleoprotein filament and the target duplex DNA was limited to a region of only about 80 bp. Taken together, this provides exciting insight into the strand-exchange mechanism.

RESULTS

A magnetic tweezers setup (Figure 1) enables control of the topological state of a single tethered double-stranded DNA molecule and monitoring the DNA end-to-end distance with nanometer resolution in real time (Strick et al., 1998). A 10 kb double-stranded DNA molecule was tethered between a glass slide and a bead in a flow cell. The molecule included a region of sequence homology to RecA-coated single-stranded DNA filaments, which in our study ranged from 359 to 1055 bp in length (see the Experimental Procedures). Strand exchange was initiated by introducing RecA-coated single-stranded DNA filaments into the flow cell. Interaction of a RecA-coated single-stranded DNA filament with the tethered duplex DNA molecule will induce changes in the structure of the tether (Figure 1A). The DNA bound by RecA is locally elongated by 50%, leading to an increase in end-to-end distance of the tethered double-stranded DNA. More significantly, changes in DNA helical twist, induced by interaction with the RecA-coated single-stranded DNA filament, can be sensitively measured by using magnetic tweezers. The tethered double-stranded DNA was negatively supercoiled by external magnets to a degree at which strand exchange is readily observed in ensemble reactions (supercoil density $\sigma \simeq -0.04$; 35 negative rotations for our 10 kb double-stranded DNA at a stretching force of 0.5 pN [Cai et al., 2001; Dasgupta and Radding, 1982; Wong et al., 1998]). Recombination-induced changes in twist will cause large changes in end-to-end distance because plectonemic supercoils are removed from the torsionally constrained double-stranded DNA molecule (Figure 1B). We thus followed strand pairing and exchange by RecA in real time via the changes in end-to-end distance of the target DNA.

Rate of Joint-Molecule Formation in the Presence of ATPγS

First, we studied the reaction for RecA-coated single-stranded DNA nucleoprotein filaments that were preassembled in the presence of ATPγS, an ATP analog that is poorly hydrolyzable. In this condition, RecA polymerizes on single-stranded DNA into stable filaments (McEntee et al., 1981) and is able to catalyze strand exchange with double-stranded DNA, despite the lack of

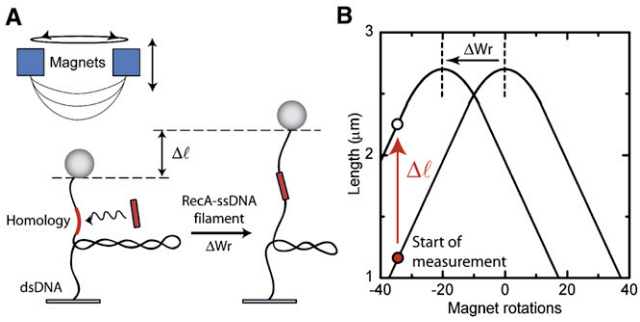

Figure 1. RecA-Mediated DNA Strand Invasion and Exchange

(A) Schematic drawing of the magnetic tweezers setup. A DNA molecule is attached at one end to the bottom of the flow cell and at the other end to a magnetic bead. This molecule can be stretched and twisted by using a pair of magnets placed above the flow cell. The bead position, and thus the end-to-end distance of the DNA molecule, is determined by using video microscopy and image analysis. In this setup, the interaction of a RecA-coated single-stranded DNA filament with a homologous duplex DNA molecule can be followed in real time because binding induces a change in end-to-end distance of the tethered molecule.

(B) Rotation of the external magnets induces a change in end-to-end distance due to the formation of plectonemic supercoils (Strick et al., 1998). Thirty-five negative plectonemic supercoils were introduced at a stretching force of 0.5 pN before initiation of the strand invasion and exchange reaction. Upon binding, a RecA-coated single-stranded DNA nucleoprotein filament partially unwinds the target double-stranded DNA molecule and therefore amplifies the signal ΔL due to the removal of negative plectonemic supercoils and therefore shifting the center of the rotation dependency of the tethered molecule toward lower numbers.

ATP hydrolysis. The final product of strand invasion with ATPγS is a joint molecule bound by RecA (Menetski et al., 1990). After RecA-coated single-stranded DNA filaments were added to the flow cell, a lag time was observed during which the length of the DNA tether did not change, followed by a steady increase in end-to-end distance (see top curve in Figure 2A). The length increase indicated joint-molecule formation due to protein-stabilized local unwinding and stretching of the homologous region of the tethered molecule. The increase progressed linearly with time, after which the end-to-end distance remained constant. The duration time τ_1 of the length increase depended linearly on the length of the homologous piece of single-stranded DNA used. Experiments were repeated multiple times (n = 5) for each length of homologous single-stranded DNA used (359, 696, and 1055 nt). Figure 3 shows a linear fit between τ_1 and homology length that yields a rate of strand pairing of 2.11 ± 0.05 nt/s at 22°C. Time τ_1 reflects the time needed to form a joint molecule over the entire homologous region.

Kinetics of Strand Invasion and Exchange in the Presence of ATP

RecA-coated single-stranded DNA nucleoprotein filaments were also preassembled and studied in the presence of ATP, which supports full biological activity. Here again, following a lag time after introduction of the RecA-coated single-stranded DNA filaments into the flow cell, the end-to-end distance of the tethered double-stranded DNA started to increase (see bottom curve in Figure 2A). However, it subsequently reached a plateau,

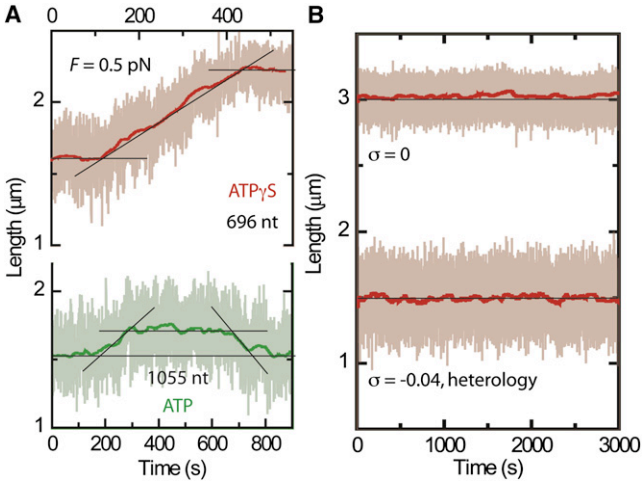

Figure 2. Interaction of a RecA-Coated Single-Stranded DNA Nucleoprotein Filament with a Homologous Duplex DNA Molecule

(A) In the presence of ATPγS, the end-to-end distance of the double-stranded DNA tether increased monotonically before reaching a plateau at which no further elongation or shortening was observed (red). In the presence of ATP, however, the end-to-end distance displayed a smaller increase and finally returned to its original level (green).

(B) Control experiments in the absence of negative supercoiling (top curve) or lacking homology between a RecA-coated single-stranded DNA nucleoprotein filament and the double-stranded DNA molecule (bottom curve) did not result in changes of the end-to-end distance in the presence of ATPγS.

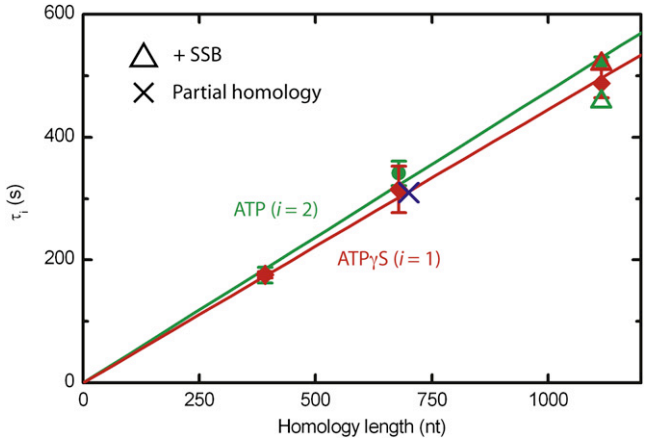

Figure 3. The Rate of Strand Invasion and Joint-Molecule Formation for Different Nucleotide Cofactors, the Presence of Single-Stranded Binding Protein, and Partial Homology

The duration time of the length increase (τ_i) induced in the double-stranded DNA tether by its interaction with a RecA-coated single-stranded DNA nucleoprotein filament scales linearly with the length of homology for both ATP ($i = 2$) and ATPγS ($i = 1$), yielding a rate of strand invasion and joint-molecule formation of 2.25 ± 0.04 (green) and 2.11 ± 0.05 (red) nt/s, respectively. RecA-coated single-stranded DNA nucleoprotein filaments formed in the presence of SSB protein (triangle) show an interaction time similar to those assembled in the absence of SSB protein. Green and red represent measurements done in the presence of, respectively, ATPγS and ATP (data are represented as mean ± SEM, n = 5). The interaction time of RecA-coated single-stranded DNA with a 5′ heterologous tail corresponds to the length of homology between invading and target DNA (cross).

followed eventually by a decrease to the initial length. We define a time τ_2 as the duration between the initial increase and the moment when the final decrease has finished. This time denotes the interaction time between a RecA-coated single-stranded DNA nucleoprotein filament and the tethered double-stranded DNA molecule. Indeed, we found that τ_2 is linearly dependent on the length of the homologous single-stranded DNA (Figure 3). The experiment was repeated multiple times (n = 5) for each length of homology, and a linear fit between interaction time and homology length yielded a rate of strand exchange of 2.25 ± 0.04 nt/s at 22°C. This value is in excellent agreement with the value of 2.0 ± 0.2 nt/s determined by extrapolation from bulk data to 22°C (Bedale and Cox, 1996). We observe that τ_1 and τ_2 for reactions done with ATPγS and ATP, respectively, were almost the same, with τ_2 slightly exceeding τ_1 (Figure 3). The similarity of these values indicates that the strand pairing rate is independent of ATP hydrolysis.

The observed changes in end-to-end distance are highly specific to RecA-coated single-stranded DNA strand invasion and exchange with homologous double-stranded DNA. Control experiments that lacked either RecA or single-stranded DNA, or that used single-stranded DNA with a complete heterologous sequence, did not yield any increase in end-to-end distance (Figure 2B, bottom curve). In the case in which the invading single-stranded DNA was partially homologous to the target duplex DNA by containing 696 nt of homologous DNA and a 359 nt heterologous 5′ end, the interaction time corresponded to the length of the homology between the two strands (repeated three times in the presence of ATPγS, Figure 3 and see Figure S1 available online), i.e., strand pairing occurred for the 3′ end homologous part but stopped at the heterologous part. Negative supercoiling was also required, as strand invasion was not detected within a reasonable time frame (3 hr) for torsionally relaxed or positively supercoiled tethered DNA molecules (Figure 2B, top curve). After the formation of a stable joint molecule with ATPγS, we attempted to complete the reaction by the addition of ATP. This appeared not to be possible, i.e., the end-to-end distance of the tethered duplex DNA molecule stayed constant and did not return to the initial length. It has been shown that RecA-double-stranded DNA nucleoprotein filaments formed in the presence of ATPγS could not be coaxed to disassemble by a change in buffer conditions from ATPγS to ATP (Galletto et al., 2006; Shibata et al., 1979; Weinstock et al., 1979). This indicates that the exchange of ATPγS and ATP is not efficient.

Influence of SSB

RecA nucleoprotein filament formation on single-stranded DNA can be stimulated by single-stranded binding (SSB) protein, because SSB removes secondary structure in single-stranded DNA (Muniyappa et al., 1984). After filament formation in the presence of SSB, RecA-coated single-stranded DNA was introduced in the flow cell. The same strand-exchange phenomena were observed as for RecA-coated single-stranded DNA in the absence of SSB (Figure 3 and Figure S2). Also the interaction times were similar, both for experiments in ATP and those in ATPγS. Under the experimental conditions we employed, the RecA-single-stranded DNA nucleoprotein filaments are thus fully

functional even in the absence of SSB. It has been reported that SSB stimulates the strand invasion and exchange reaction when single-stranded DNA is present in excess over RecA (McEntee et al., 1980). In our experimental conditions, however, RecA is present in small excess over single-stranded DNA to ensure complete coverage, removing the need for the stimulatory effect of SSB (Kahn and Radding, 1984).

Structure of the Joint Molecule

The experiments with ATPγS were analyzed to determine the helical pitch of the protein-bound DNA intermediate formed. The increase in end-to-end distance of the DNA tether during joint-molecule formation (Figure 2A) can be attributed to a combination of local stretching and unwinding of the tethered DNA molecule. Unwinding was independently confirmed by measuring the end-to-end distance of the final construct as a function of externally applied magnetic rotations. As shown in Figure 4A, invasion of a 1055 nt RecA-coated single-stranded DNA nucleoprotein filament resulted in a change in the writhe ΔWr of the tethered duplex molecule of ΔWr = −32. Importantly, the shift in rotational offset was linearly dependent on the length of homology (Figure 4B). This linear fit is strong evidence that ΔWr is proportional to the length of sequence homology. Additional RecA binding to duplex DNA distal to the site of DNA pairing (Kiianitsa and Stasiak, 1997; Voloshin and Camerini-Otero, 1997) is unlikely, because this would yield an offset at zero length of homology, which is not observed. Furthermore, we would not expect this distal binding, if it occurs, to be similar in all experiments. The experiment was repeated multiple times (n = 5) for each length of homology used. A linear fit of ΔWr versus homology length yielded a slope of 0.0278 ± 0.0011 turns per nucleotide. Assuming a uniform structure within the homologous regions, this indicates that the protein-bound joint molecule has a helical pitch h of 14.6 ± 0.2 bp per turn, using $1/h = 1/h_{DNA} - \Delta Wr$ and h_{DNA} = 10.4 bp per turn. This pitch characterizes the structure that is formed after invasion of the RecA-coated single-stranded DNA into the double-stranded DNA but before ATP-hydrolysis-stimulated RecA dissociation has occurred.

What is the structure of the protein-bound intermediate that is formed during strand invasion in the presence of ATPγS? Our experimental result for the helical pitch can be compared with a variety of proposed structures. Straightforward coating of double-stranded DNA by RecA yields RecA-coated double-stranded DNA filaments that have a helical pitch of 18.6 bp per turn (Stasiak and Dicapua, 1982). This would correspond to a slope of $(1/10.4 - 1/18.6) = 0.0424$ turns per nucleotide (Figure 4B, dashed line), which is clearly different from the 0.0278 turns per nucleotide that we observed for joint molecules. The structure of DNA in the joint molecule thus differs from that of the well-studied nucleoprotein filament of RecA-coated double-stranded DNA. Alternatively, the joint molecule could include a displaced loop (D loop) in which the invading strand has formed Watson-Crick base pairs with its homologous partner, while its complementary strand is unwound and expelled (Zhou and Adzuma, 1997). A local bubble in the tethered DNA molecule where the DNA is completely unwound would yield a slope of 0.096 turns per nucleotide, because one helical turn is removed for every 10.4 bp (Figure 4B, dotted line). Again, this structure is clearly incompatible with the data. Molecular modeling of RecA-bound three-stranded structures suggests a base-base distance that is elongated by 50% and a twist per base pair that has changed to 23 ± 2°, corresponding to a helical pitch of 15.7 ± 1.4 bp per turn (Bertucat et al., 1999; Xiao and Singleton, 2002). This is in good agreement with the value of 14.6 ± 0.2 bp per turn that we experimentally determined in the presence of ATPγS. This may be related to the reported helical pitch variation for RecA protein in DNA filaments (Yu et al., 2001). We thus

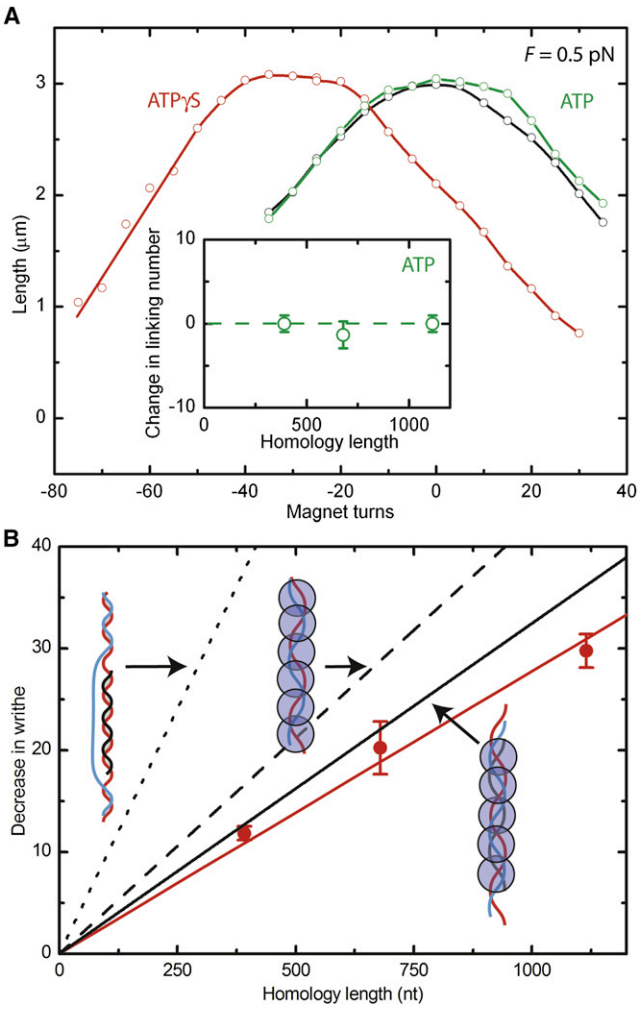

Figure 4. Change in Writhe during Joint-Molecule Formation

(A) After the formation of a joint molecule in the presence of ATPγS, a ΔWr was observed for the tethered duplex DNA molecule. In the case of 1055 nt of homology, the rotational offset was changed by −32 (red). After the formation of a joint molecule in the presence of ATP, however, the writhe was unchanged (green), independent of the length of homology used (see inset).

(B) The ΔWr observed with ATPγS scales linearly with the length of homology yielding a slope of 0.0278 ± 0.0011 turns per nucleotide, corresponding to the formation of a structure with 14.6 ± 0.2 bp per turn (red line). The data are represented as mean ± SEM (n = 5). The dotted line depicts the expected result for a complete unwinding during joint-molecule formation. The dashed line corresponds to the structure of a RecA-coated double-stranded DNA filament. The black solid line denotes the result of a RecA-bound three-strand structure derived from molecular modeling.

conclude that joint-molecule formation occurs through a protein-bound intermediate with the same helical pitch and rise per base pair as extracted from molecular modeling simulations (Bertucat et al., 1999; Zhurkin et al., 1994).

Length of DNA Synapsis during Strand Exchange

It is remarkable that the double-stranded DNA end-to-end distance during strand invasion and exchange in the presence of ATP increased to a constant value of ΔL = 134 ± 11 nm (n = 15) independent of the length of homology used between 359 and 1055 nt. We interpret this as a signature of the dynamics of the synapsis in the strand-exchange process with equal rates for strand invasion and RecA release upon ATP hydrolysis. The recombination process can be depicted as follows (Figure 5): the invading end of a RecA-coated single-stranded DNA filament elongates and opens the tethered target double-stranded DNA molecule forming a protein-bound intermediate, where the associated change in twist consumes writhe, thus increasing the end-to-end distance. At the trailing end of the invaded region, RecA dissociates when ATP is hydrolyzed (Fulconis et al., 2006), relaxing the local stretching and twisting. Subsequently, the end-to-end distance remains constant as the synapsis between the RecA-coated single-stranded DNA filament and the double-stranded DNA molecule travels along the region of homology while continuously performing strand exchange. We can determine the length n of the synapsed region, based on the constant length change ΔL in the tethered double-stranded DNA during strand exchange, as

$$n(d_{\text{RecA-DNA}} - d_{\text{DNA}}) + n\Delta\varphi\Delta l = \Delta L, \quad (1)$$

where $d_{\text{RecA-DNA}}$ = 0.51 nm (Bertucat et al., 1999) and d_{DNA} = 0.34 nm are the base pair rise in, respectively, the protein-bound intermediate and B-DNA, $\Delta\varphi$ the change in twist between the two structures, and Δl the increase in end-to-end distance for the removal of a single negative plectonemic supercoil. At the 0.5 pN force exerted, the latter amounts to Δl = 55 ± 2 nm (the left slope of the black curve in Figure 4A). For a change in twist of 0.028 turns per nucleotide in the protein-bound intermediate, Equation 1 leads to n = 79 ± 6 bp of the double-stranded DNA tether. We thus obtain the length of the active synapsis between a RecA-coated single-stranded DNA nucleoprotein filament and its homologous duplex partner during strand exchange, which amounts to a surprisingly low value of only about 80 bp, even when the homology length is much longer.

Structure of DNA after Strand Exchange

After strand exchange is completed in the presence of ATP, the end-to-end distance is the same as the starting double-stranded DNA. This is a priori unexpected, since the structure of the tether has locally changed in the recombination process. In the presence of ATP, we also found that the writhe of the tethered molecule was unchanged after strand invasion and exchange was completed (Figure 4A and its inset), i.e., the twist as well as the end-to-end distance is equal to the starting DNA. The expulsion of one strand of the original double-stranded DNA in the exchange process would induce a large ΔWr of the tethered double-stranded DNA. However, this can be compensated for

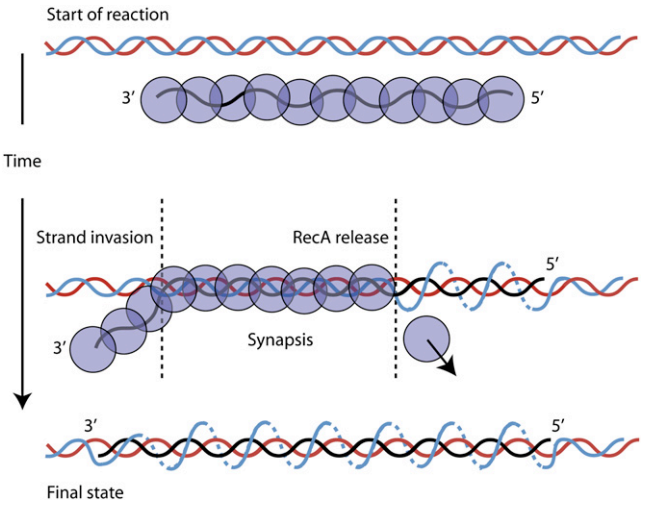

Figure 5. Schematic Representation of the Strand Invasion and Exchange Reaction by RecA

Interactions occur between a RecA-coated single-stranded DNA nucleoprotein filament (purple circles—black line) and a double-stranded DNA molecule (blue-red). During strand exchange, a window of synapsis of 79 ± 6 nt in length travels along the length of homology (toward the left in the cartoon, 5′ to 3′ with respect to the invading single strand). The direction of strand exchange and of RecA dissociation is consistent with established behavior of RecA and not determined specifically from our data. The final structure after strand exchange is obtained when RecA dissociates and the displaced single strand (blue) wraps around the newly formed duplex DNA. The exact structure of the D wrap has not yet been determined. Although drawn in a regular helix around the double strand, the displaced single strand is flexible and may not have a defined structure.

by wrapping the displaced strand around the newly formed duplex, a structure best described as a D wrap. The contour length of this path can be estimated as $L_{\text{ssDNA}} = \sqrt{L_{\text{dsDNA}}^2 + (2\pi mR)^2}$, where L_{dsDNA} is the length of the newly formed double-stranded DNA, m the number of rotations, and R the radius of the double-stranded DNA molecule. The number of rotations is equal to the number of helical turns in the newly formed duplex DNA, $m = L_{\text{dsDNA}}/3.5\,\text{nm}$. Assuming a radius of 0.76 nm (Saenger, 1984), a base-base distance in double-stranded DNA of 0.34 nm, we obtain a contour length of the displaced strand of 0.58 nm per nucleotide, which fits the value for free single-stranded DNA (Smith et al., 1996). Consideration of the molecular dimensions thus shows that the length of the displaced DNA strand is long enough to wrap itself around the newly formed duplex DNA, thereby avoiding any changes in twist.

Given the same DNA end-to-end distance before and after the strand-exchange reaction with ATP, one might question whether this reaction actually occurred. The presence of newly base-paired partner strands after the reaction is unambiguously demonstrated in the following experiments. First, in bulk, strand exchange was carried out with a RecA-coated single-stranded oligonucleotide, including the recognition sequence for restriction enzyme ApaLI, and a double-stranded plasmid in the same conditions as those in the magnetic tweezers (Figure 6A, left panel). After strand exchange, all of the invaded single-stranded DNA oligonucleotide was cleaved by ApaLI (Figure 6A, right panel),

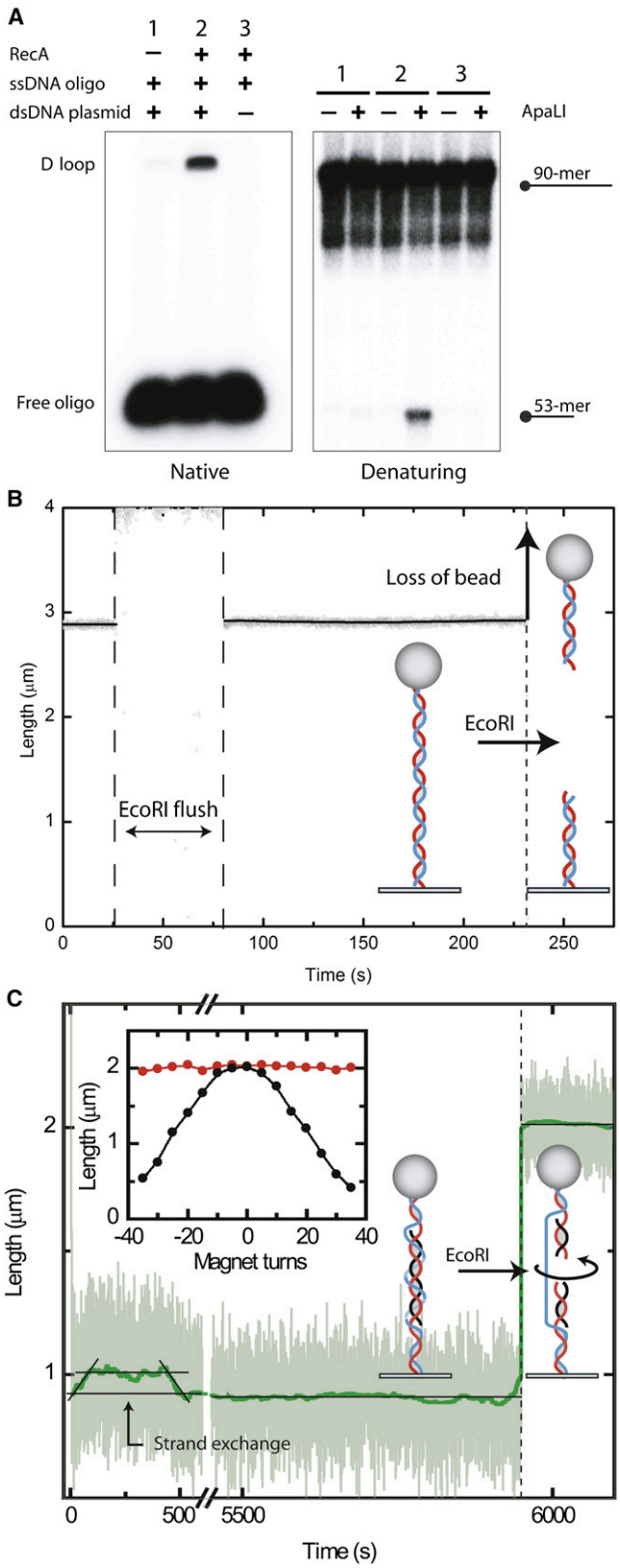

Figure 6. Change in Structure after Strand Exchange

(A) Restriction enzyme cleavage of the invading strand after D loop formation by RecA. (Left panel) D loop reactions were performed using a 5′ end-radiolabeled oligonucleotide (90-mer) homologous to a region of pUC19 plasmid encompassing an ApaLI restriction site. Reaction products were resolved by electrophoresis through a native agarose gel. (Right panel) After the D loop reaction, samples numbered as in the right panel before and after treatment with ApaLI were resolved by electrophoresis in a denaturing acrylamide gel.

(B) Addition of a restriction enzyme to the double-stranded DNA construct in the magnetic tweezers. Before strand exchange, addition of a restriction enzyme with its recognition sequence inside the region of homology led to the loss of bead tracking because the tethered DNA molecule was cut.

(C) After strand exchange by RecA in the presence of ATP, however, the restriction enzyme EcoRI did not cut the DNA tether but rather released the torsional constraint. The end-to-end distance was seen to increase due to the release of the negative plectonemic supercoils by rotation of one strand around the other. The inset shows the rotation-dependent behavior before (black) and after (red) the treatment with the restriction enzyme. Before introduction of the restriction enzyme in the flow cell, the tethered DNA molecule shows a torsionally constrained behavior, whereas after treatment the molecule is torsionally unconstrained, yielding the same end-to-end distance for various applied rotations.

indicating that this single DNA strand was now in a double-stranded form recognized and cleaved by a restriction enzyme. Similarly, in the magnetic tweezers setup, a recognition site for the restriction enzyme EcoRI was located within the region of homology. In the absence of invaded single-stranded DNA—thus without any strand exchange—the DNA tether was simply broken upon adding EcoRI (Figure 6B). A similar behavior was observed for negatively supercoiled DNA (data not shown). If the invaded single-stranded DNA is present in a new duplex after exchange, however, the DNA tether should not break but should become torsionally unconstrained as the displaced strand stays intact and holds the construct together, while the paired strand is broken (see inset of Figure 6B) (Voloshin and Camerini-Otero, 1997). This was indeed observed (n = 3) in the magnetic tweezers (Figures 6B and 6C), indicating that strand exchange had occurred and resulted in new base-paired partners in the tethered DNA, with one strand of the tether paired with the invading single strand in a structure recognized by a restriction enzyme. The displaced single strand remains wrapped around the newly formed duplex the same number of times as it was when paired. This flexible single strand need not have a regular or defined structure and apparently does not hinder access of a restriction enzyme. Control experiments in which a recognition sequence was placed outside the region of homology resulted in cutting of the DNA tether independent of strand exchange.

DISCUSSION

In summary, we observed strand invasion and joint-molecule formation by RecA in real time on single DNA molecules. The overall exchange rates are similar to those determined in ensemble assays, but our single-molecule approach revealed key details of the kinetics and the DNA structures formed during strand exchange. We show that during joint-molecule formation a protein-bound three-stranded structure is formed which, assuming uniform structure along the paired homology, has a helical pitch of 14.6 ± 0.2 bp per turn. Furthermore, the length of the synapsis

where strand invasion and exchange occurs is only 79 ± 6 bp long. Finally, the displaced strand is wrapped around the newly formed heteroduplex DNA.

Our observations match well with reported properties for RecA strand invasion and exchange. In contrast, the length decreases reported by others are unexpected and unexplained (Fulconis et al., 2006). This decrease in end-to-end distance was attributed to the formation of a D loop structure. As discussed above, the formation of a D loop structure would remove some of the negatively supercoiled plectonemes increasing the end-to-end distance. The authors also suggest that interaction between the tethered molecule and the glass surface could cause the length decrease observed. Such behavior is independent of the strand invasion and exchange reaction induced by RecA. Fulconis et al. also observed an increase in end-to-end distance in the presence of ATPγS, but this did not correlate with the length of homology used.

The strand invasion and exchange reaction in the presence of ATP has been shown to have a 5′ to 3′ directionality (Cox and Lehman, 1981; Kahn et al., 1981; West et al., 1981). In a recent single-molecule experiment, the assembly and dissociation rates during filament formation were studied for both ends of the nucleoprotein filament (Joo et al., 2006). The nucleoprotein filament extends at the 3′ end, while dissociation occurs at the 5′ end due to differences in the assembly and dissociation rates at both ends (reviewed in Kowalczykowski, 1991). At the trailing end of the strand invasion reaction, RecA would disassemble. The picture we sketched in Figure 5 is consistent with the described assembly/disassembly behavior of RecA.

In the presence of ATPγS, strand invasion and exchange reactions lack distinct polarity (Jain et al., 1994; Shan et al., 1996), and the invasion can occur from either end of the invading nucleoprotein filament. The behavior observed in our experiments with ATPγS is inconsistent with bidirectional strand pairing, because we always see a simple linear increase in the end-to-end distance. If strand invasion would be bidirectional, the increase in end-to-end distance would contain two distinct slopes expected to differ by a factor two.

Notably, all strand-exchange reactions that we observed continued to completion once initiated. We observed no partial recombination processes or reversals. In bulk experiments, RecA has been shown to perform full strand exchange between circular single-stranded DNA and linear double-stranded DNA, yielding a total conversion into nicked circular double-stranded DNA and linear single-stranded DNA (Bianchi et al., 1983; Dasgupta et al., 1980). This is a signature that 100% of the invading single-stranded DNA substrate underwent base-pair exchange. In the presence of both ATP and ATPγS, there was a time lag before strand invasion started during which the end-to-end distance did not change. The latter implies that in the step of homology search, prior to strand exchange, the RecA-coated single-stranded DNA nucleoprotein filament is not interacting with the tethered double-stranded DNA in a way that yielded a signal beyond our detection limit. Our observations therefore place upper limits on structural disturbances that might occur during the so-called homology search. For instance, opening of the helical structure of the tethered duplex DNA molecule might be involved in the homology search but would have been sensitively detected in our experiments by plectoneme release and the associated increase in DNA tether length. Length changes induced during homology search that exceed one standard deviation of the intrinsic noise (σ_l) of the Brownian motion of the magnetic bead at the force exerted can be estimated as $\Delta L \gtrsim \sigma_l/\sqrt{tf_c}$, where t is the time in which a D loop is formed and f_c the corner frequency (0.82 Hz) of the power spectrum at the force exerted of the magnetic tweezers setup. Our RMS noise level of σ_l = 75 nm at the low force of 0.5 pN then puts an upper bound for ΔWr of 1.5 turns (unwinding of 16 bp) for a 1 s interaction time between a RecA-coated single-stranded DNA nucleoprotein filament and the double-stranded DNA tether.

The product of strand exchange has the invading single strand base paired to the partner in a B-form duplex, with the displaced strand unpaired but wrapped around the new duplex. The DNA structures formed during joint-molecule formation show that it occurs through a protein-bound intermediate with (average) helical properties different from both B-form DNA and RecA-coated double-stranded DNA. Subsequently, the apparent conformational transition from the protein-bound intermediate to B-form DNA under the influence of ATP hydrolysis may help to drive the reaction toward exchange of strands in favor of reversal. By analyzing reactions in real time on single molecules, we showed that, unexpectedly, exchange of strands occurs with an active synapsis of only 79 ± 6 bp. This implies that similar rates of strand invasion and protein dissociation result in a synaptic region of constant length moving along the region of homology while continuously performing strand exchange.

EXPERIMENTAL PROCEDURES

DNA Substrates

Construction of pBluescr1234

A DNA construct named pBluescr1234 was made from pBluescriptII SK+ (Stratagene) by sequentially inserting four PCR fragments derived from λDNA into the multiple cloning site of the vector. PCR fragment 1 (forward primer, AAAATCTAGAAGTTCAGGAAGCGGTGATGCTG; reverse primer, AAAAGAGCTCTTGGGCGGTTGTGTACATCGAC) spans base pairs 4236–6137. After digestion with the corresponding restriction enzymes (underlined in the primer sequences), it was cloned between the XbaI and the SacI sites of the vector. PCR fragment 2 (forward primer, AAAAGAATTCGGTGACCCTTACGC GAATCC; reverse primer, AAAATCTAGAGGCTTCAGCGACCTTGTCC) spans base pairs 9043–11201. After digestion with the corresponding restriction enzymes, it was cloned between the EcoRI and the XbaI sites of the vector. PCR fragment 3 (forward primer, AAAAGAATTCCTCAGCGACGCAGGGGACCTGC AGG; reverse primer, AAAACTCGAGTGCCGTTGTAACCGGTCATC) spans base pairs 2826–4726. After digestion with the corresponding restriction enzymes, it was cloned between the EcoRI and the XhoI sites of the vector. PCR fragment 4 (forward primer, AAAAGGTACCAGTTCAGGAAGCGGTGATG CTG; reverse primer, AAAAACTCGAGCAGCAACCGCAAGAATGC) spans base pairs 4236–5925. After digestion with the corresponding restriction enzymes, it was cloned between the KpnI and the XhoI sites of the vector.

Construction of pBluescr134M13

A DNA construct named pBluescr134M13 was made from pBluescriptII SK+ (Stratagene) by sequentially inserting three PCR fragments derived from λDNA (see above for PCR fragments 1, 3, and 4) and one PCR fragment from m13mp18 (New England Biolabs). PCR fragment M13 (forward primer, AAAAGAATTCTGTGGAATGCTACAGGCGTTG; reverse primer, AAAAACTAG TAGGGCTTAATTGAGAATCG) spans base pairs 1739–3761. After digestion with the corresponding restriction enzymes, it was cloned between the EcoRI and the SpeI site of the vector.

Production of DNA Substrates for Magnetic Tweezers Experiments

For assays involving complete homologous DNA, pBluescr1234 was cleaved with PciI and SacI, resulting in a 10 kb linear fragment. For experiments involving partial homologous DNA, pBluescr134M13 was cleaved with KpnI and NgoMIV, resulting in a 10 kb linear fragment. Both fragments were ligated to two 700 bp PCR fragments, one containing several biotin-modified dUTP bases and the other PCR fragment containing several digoxigenin-modified dUTP bases. Using the magnetic tweezers, we selected molecules that were rotationally constrained. For experiments involving rotationally constrained but heterologous DNA, psFV1 was prepared as described previously (van der Heijden et al., 2005).

Production of Single-Stranded DNA

Three different lengths of single-stranded DNA fragments were prepared as follows. First, a double-stranded 1055 bp DNA fragment containing the nicking endonuclease Nb.BbvCI recognition site (GCTGAGG) was produced by PCR by using pBluescr1234 (see above) as a template from 1251 to 2305. After purification, the PCR fragment was treated with the nicking endonuclease Nb.BbvCI at 37°C for 1 hr. Subsequently, the nicked 1055 bp PCR fragment was loaded on an alkaline agarose gel to generate single-stranded DNA (Sambrook et al., 1989). Three different lengths of single-stranded DNA (359, 696, and 1055 nt) were obtained after purification by gel extraction.

Magnetic Tweezers

The magnetic tweezers setup used in these experiments is described by Strick et al. (1998). By image processing, 5 nm position accuracy of the bead was obtained in all three dimensions. In plots showing DNA extension, the points presented are the raw data acquired at 60 Hz. When shown, solid lines correspond to data filtered at 0.033 Hz. To exclude the effect of thermal drift, all positions were measured relative to a 3.2 μm polystyrene bead (Bang Laboratories, Carmel, IN) fixed to the bottom of the flow cell.

Flow Cell

Polystyrene beads as well as DNA constructs carrying a magnetic bead at one end were anchored to the bottom of a flow cell as described elsewhere (van Noort et al., 2004). The force-extension curve of single DNA molecules was measured (Figure 1B). After confirmation of the correct contour and persistence lengths, experiments were started by addition of RecA-coated single-stranded DNA filaments. All reactions were carried out at 22°C.

RecA/DNA Reactions

The flow-cell final volume was approximately 100 μl. All reactions were done in 20 mM Tris-HCl (pH 7.5), 10 mM $MgCl_2$, and 1 mM ATP or ATPγS. First, RecA-coated single-stranded DNA nucleoprotein filaments were preassembled before introduction in the flow cell. In the experiments including SSB, 1.0 μM single-stranded DNA (in nucleotides) and 50 nM SSB (Promega) were incubated in the indicated reaction buffer at 37°C for 10 min. After this, 0.4 μM RecA (New England Biolabs) was added and incubated at 37°C for 30 min. Subsequently, the RecA-coated single-stranded DNA was diluted in the reaction buffer to 0.3 nM (in DNA molecules). Interaction of a RecA-coated single-stranded DNA filament with the tethered DNA molecule was monitored through measurement of the height of the magnetic bead. The restriction enzymes AseI and EcoRI (New England Biolabs), respectively 1 and 2 units, were added in the flow cell to probe the structure of the DNA tether before and after strand exchange.

D Loop Assay

RecA (1 μM) was incubated with ^{32}P-labeled single-stranded DNA (90-mer, SK3) (Mazin et al., 2000) (3 μM) in 50 mM Tris-HCl (pH 7.5), 1 mM ATP, 100 μg/ml BSA, 1 mM DTT, 30 mM KCl (added with the protein stock), and 10 mM $MgCl_2$ for 5 min at 37°C to allow filament formation. D loop formation was initiated by addition of 90 μM pUC19 double-stranded DNA (in nucleotides). After incubation at 37°C for 20 min, an aliquot was taken from the reaction mixture and deproteinized by incubation for 15 min at 37°C with 1.2 mg/ml final of Proteinase K and 1% (w/v) SDS. Reaction products were fractionated by 0.6% agarose gel electrophoresis in Tris-borate buffer. To the remainder of the reaction mixture, 10 units of the restriction enzyme ApaLI (New England Biolabs) were added and further incubated for 30 min at 37°C. Reactions were stopped by addition of 1 volume of 50 mM EDTA and 90% formamide and resolved by denaturing urea/acrylamide gel electrophoresis. Signals were captured by phosphorimaging using a Typhoon scanner and quantified using ImageQuant version 5.2 (Molecular Dynamics).

SUPPLEMENTAL DATA

Supplemental Data include two figures and can be found with this article online at http://www.molecule.org/cgi/content/full/30/4/530/DC1/.

ACKNOWLEDGMENTS

We thank Ya-Hui Chien and Peter Veenhuizen for technical assistance and Koen Besteman, Frank van Heesch, Tommy Holthausen, Stephen Kowalczykowski, Hendrikje van Leest, Marijn van Loenhout, Ralf Seidel, and Andrzej Stasiak for helpful discussions. This work was supported by the "Stichting voor Fundamenteel Onderzoek der Materie (FOM)" and by the "Nederlandse Organisatie voor Wetenschappelijk Onderzoek (NWO)," the Netherlands Genomic Initiative/NWO, and the European Commission (IP 512113 and IP 503259).

Received: May 28, 2007
Revised: November 2, 2007
Accepted: March 7, 2008
Published: May 22, 2008

REFERENCES

Bazemore, L.R., Folta-Stogniew, E., Takahashi, M., and Radding, C.M. (1997a). RecA tests homology at both pairing and strand exchange. Proc. Natl. Acad. Sci. USA *94*, 11863–11868.

Bazemore, L.R., Takahashi, M., and Radding, C.M. (1997b). Kinetic analysis of pairing and strand exchange catalyzed by RecA—detection by fluorescence energy transfer. J. Biol. Chem. *272*, 14672–14682.

Bedale, W.A., and Cox, M.M. (1996). Evidence for the coupling of ATP hydrolysis to the final (extension) phase of RecA protein-mediated DNA strand exchange. J. Biol. Chem. *271*, 5725–5732.

Bertucat, G., Lavery, R., and Prevost, C. (1999). A molecular model for RecA-promoted strand exchange via parallel triple-stranded helices. Biophys. J. *77*, 1562–1576.

Bianchi, M., Dasgupta, C., and Radding, C.M. (1983). Synapsis and the formation of paranemic joints by *Escherichia coli* RecA-protein. Cell *34*, 931–939.

Cai, L.P., Marquardt, U., Zhang, Z.Q., Taisey, M.J., and Chen, J.H. (2001). Topological testing of the mechanism of homology search promoted by RecA protein. Nucleic Acids Res. *29*, 1389–1398.

Cox, M.M., and Lehman, I.R. (1981). Directionality and polarity in RecA protein-promoted branch migration. Proc. Natl. Acad. Sci. USA *78*, 6018–6022.

Dasgupta, C., and Radding, C.M. (1982). Lower fidelity of RecA protein catalyzed homologous pairing with a superhelical substrate. Nature *295*, 71–73.

Dasgupta, C., Shibata, T., Cunningham, R.P., and Radding, C.M. (1980). The topology of homologous pairing promoted by RecA protein. Cell *22*, 437–446.

Ellouze, C., Norden, B., and Takahashi, M. (1997). Dissociation of non-complementary second DNA from RecA filament without ATP hydrolysis: mechanism of search for homologous DNA. J. Biochem. (Tokyo) *121*, 1070–1075.

Folta-Stogniew, E., O'Malley, S., Gupta, R., Anderson, K.S., and Radding, C.M. (2004). Exchange of DNA base pairs that coincides with recognition of homology promoted by *E. coli* RecA protein. Mol. Cell *15*, 965–975.

Frank-Kamenetskii, M.D., and Mirkin, S.M. (1995). Triplex DNA structures. Annu. Rev. Biochem. *64*, 65–95.

Fulconis, R., Mine, J., Bancaud, A., Dutreix, M., and Viovy, J.L. (2006). Mechanism of RecA-mediated homologous recombination revisited by single molecule nanomanipulation. EMBO J. *25*, 4293–4304.

Galletto, R., Amitani, I., Baskin, R.J., and Kowalczykowski, S.C. (2006). Direct observation of individual RecA filaments assembling on single DNA molecules. Nature *443*, 875–878.

Gumbs, O.H., and Shaner, S.L. (1998). Three mechanistic steps detected by FRET after presynaptic filament formation in homologous recombination. ATP hydrolysis required for release of oligonucleotide heteroduplex product from RecA. Biochemistry *37*, 11692–11706.

Jain, S.K., Cox, M.M., and Inman, R.B. (1994). On the role of ATP hydrolysis in RecA protein-mediated DNA strand exchange. 3. Unidirectional branch migration and extensive hybrid DNA formation. J. Biol. Chem. *269*, 20653–20661.

Joo, C., McKinney, S.A., Nakamura, M., Rasnik, I., Myong, S., and Ha, T. (2006). Real-time observation of RecA filament dynamics with single monomer resolution. Cell *126*, 515–527.

Kahn, R., and Radding, C.M. (1984). Separation of the presynaptic and synaptic phases of homologous pairing promoted by RecA protein. J. Biol. Chem. *259*, 7495–7503.

Kahn, R., Cunningham, R.P., Dasgupta, C., and Radding, C.M. (1981). Polarity of heteroduplex formation promoted by Escherichia-coli RecA protein. Proc. Natl. Acad. Sci. USA *78*, 4786–4790.

Kiianitsa, K., and Stasiak, A. (1997). Helical repeat of DNA in the region of homologous pairing. Proc. Natl. Acad. Sci. USA *94*, 7837–7840.

Kowalczykowski, S.C. (1991). Biochemistry of genetic-recombination: energetics and mechanism of DNA strand exchange. Annu. Rev. Biophys. Biophys. Chem. *20*, 539–575.

Mazin, A.V., Zaitseva, E., Sung, P., and Kowalczykowski, S.C. (2000). Tailed duplex DNA is the preferred substrate for Rad51 protein-mediated homologous pairing. EMBO J. *19*, 1148–1156.

McEntee, K., Weinstock, G.M., and Lehman, I.R. (1980). RecA protein-catalyzed strand assimilation—stimulation by Escherichia-coli single-stranded DNA-binding protein. Proc. Natl. Acad. Sci. USA *77*, 857–861.

McEntee, K., Weinstock, G.M., and Lehman, I.R. (1981). Binding of the RecA protein of Escherichia-coli to single-stranded and double-stranded DNA. J. Biol. Chem. *256*, 8835–8844.

Menetski, J.P., Bear, D.G., and Kowalczykowski, S.C. (1990). Stable DNA heteroduplex formation catalyzed by the Escherichia-coli RecA protein in the absence of ATP hydrolysis. Proc. Natl. Acad. Sci. USA *87*, 21–25.

Muniyappa, K., Shaner, S.L., Tsang, S.S., and Radding, C.M. (1984). Mechanism of the concerted action of RecA protein and helix-destabilizing proteins in homologous recombination. Proc. Natl. Acad. Sci. USA *81*, 2757–2761.

Saenger, W. (1984). Principles of Nucleic Acid Structure (New York, N.Y.: Springer-Verlag).

Sambrook, J., Fritsch, E.F., and Maniatis, T. (1989). Molecular Cloning: A Laboratory Manual, Second Edition (Cold Spring Harbor, N.Y.: Cold Spring Harbor Laboratory).

Shan, Q., Cox, M.M., and Inman, R.B. (1996). DNA strand exchange promoted by RecA K72R—two reaction phases with different Mg^{2+} requirements. J. Biol. Chem. *271*, 5712–5724.

Shibata, T., Cunningham, R.P., Dasgupta, C., and Radding, C.M. (1979). Homologous pairing in genetic-recombination: complexes of RecA-protein and DNA. Proc. Natl. Acad. Sci. USA *76*, 5100–5104.

Smith, S.B., Cui, Y.J., and Bustamante, C. (1996). Overstretching B-DNA: the elastic response of individual double-stranded and single-stranded DNA molecules. Science *271*, 795–799.

Stasiak, A., and Dicapua, E. (1982). The helicity of DNA in complexes with RecA protein. Nature *299*, 185–186.

Strick, T.R., Allemand, J.F., Bensimon, D., and Croquette, V. (1998). Behavior of supercoiled DNA. Biophys. J. *74*, 2016–2028.

van der Heijden, T., van Noort, J., van Leest, H., Kanaar, R., Wyman, C., Dekker, N., and Dekker, C. (2005). Torque-limited RecA polymerization on dsDNA. Nucleic Acids Res. *33*, 2099–2105.

van Noort, J., Verbrugge, S., Goosen, N., Dekker, C., and Dame, R.T. (2004). Dual architectural roles of HU: formation of flexible hinges and rigid filaments. Proc. Natl. Acad. Sci. USA *101*, 6969–6974.

Voloshin, O.N., and Camerini-Otero, R.D. (1997). The duplex DNA is very underwound in the three-stranded RecA protein-mediated synaptic complex. Genes Cells *2*, 303–314.

Weinstock, G.M., Mcentee, K., and Lehman, I.R. (1979). ATP-dependent renaturation of DNA catalyzed by the RecA protein of Escherichia-coli. Proc. Natl. Acad. Sci. USA *76*, 126–130.

West, S.C., Cassuto, E., and Howard-Flanders, P. (1981). Heteroduplex formation by RecA protein—polarity of strand exchanges. Proc. Natl. Acad. Sci. USA *78*, 6149–6153.

Wong, B.C., Chiu, S.K., and Chow, S.A. (1998). The role of negative superhelicity and length of homology in the formation of paranemic joints promoted by RecA protein. J. Biol. Chem. *273*, 12120–12127.

Wyman, C., and Kanaar, R. (2004). Homologous recombination: down to the wire. Curr. Biol. *14*, R629–R631.

Xiao, J., and Singleton, S.F. (2002). Elucidating a key intermediate in homologous DNA strand exchange: structural characterization of the RecA-triple-stranded DNA complex using fluorescence resonance energy transfer. J. Mol. Biol. *320*, 529–558.

Yu, X., Jacobs, S.A., West, S.C., Ogawa, T., and Egelman, E.H. (2001). Domain structure and dynamics in the helical filaments formed by RecA and Rad51 on DNA. Proc. Natl. Acad. Sci. USA *98*, 8419–8424.

Yu, X., VanLoock, M.S., Yang, S., Reese, J.T., and Egelman, E.H. (2004). What is the structure of the RecA-DNA filament? Curr. Protein Pept. Sci. *5*, 73–79.

Zhou, X.H., and Adzuma, K. (1997). DNA strand exchange mediated by the Escherichia coli RecA protein initiates in the minor groove of double-stranded DNA. Biochemistry *36*, 4650–4661.

Zhurkin, V.B., Raghunathan, G., Ulyanov, N.B., Camerini-Otero, R.D., and Jernigan, R.L. (1994). A parallel DNA triplex as a model for the intermediate in homologous recombination. J. Mol. Biol. *239*, 181–200.